

neuro2vec: Masked Fourier Spectrum Prediction for Neurophysiological Representation Learning

Di Wu
wudi@westlake.edu.cn
Westlake University
Hangzhou, Zhejiang, China

Jie Yang
yangjie@westlake.edu.cn
Westlake University
Hangzhou, Zhejiang, China

Siyuan Li
lisiyuan@westlake.edu.cn
Westlake University
Hangzhou, Zhejiang, China

Mohamad Sawan
sawan@westlake.edu.cn
Westlake University
Hangzhou, Zhejiang, China

ABSTRACT

Extensive data labeling on neurophysiological signals is often prohibitively expensive or impractical, as it may require particular infrastructure or domain expertise. To address the appetite for data of deep learning methods, we present for the first time a Fourier-based modeling framework for self-supervised pre-training of neurophysiology signals. The intuition behind our approach is simple: frequency and phase distribution of neurophysiology signals reveal the underlying neurophysiological activities of the brain and muscle. Our approach first randomly masks out a portion of the input signal and then predicts the missing information from either spatiotemporal or the Fourier domain. Pre-trained models can be potentially used for downstream tasks such as sleep stage classification using electroencephalogram (EEG) signals and gesture recognition using electromyography (EMG) signals. Unlike contrastive-based methods, which strongly rely on carefully hand-crafted augmentations and siamese structure, our approach works reasonably well with a simple transformer encoder with no augmentation requirements. By evaluating our method on several benchmark datasets, including both EEG and EMG, we show that our modeling approach improves downstream neurophysiological related tasks by a large margin.

CCS CONCEPTS

• **Human-centered computing** → HCI theory, concepts and models; • **Computing methodologies** → Cognitive science.

KEYWORDS

Self-supervised, pre-training, neurophysiological signals, Fourier transform, masked autoencoding

ACM Reference Format:

Di Wu, Siyuan Li, Jie Yang, and Mohamad Sawan. 2022. neuro2vec: Masked Fourier Spectrum Prediction for Neurophysiological Representation Learning. In *Proceedings of Make sure to enter the correct conference title from your*

Permission to make digital or hard copies of all or part of this work for personal or classroom use is granted without fee provided that copies are not made or distributed for profit or commercial advantage and that copies bear this notice and the full citation on the first page. Copyrights for components of this work owned by others than ACM must be honored. Abstracting with credit is permitted. To copy otherwise, or republish, to post on servers or to redistribute to lists, requires prior specific permission and/or a fee. Request permissions from permissions@acm.org.
Conference acronym 'XX, 10-14 Oct., 2022, Lisbon, Portugal

© 2022 Association for Computing Machinery.
ACM ISBN 978-1-4503-XXXX-X/18/06...\$15.00
<https://doi.org/XXXXXXXX.XXXXXXX>

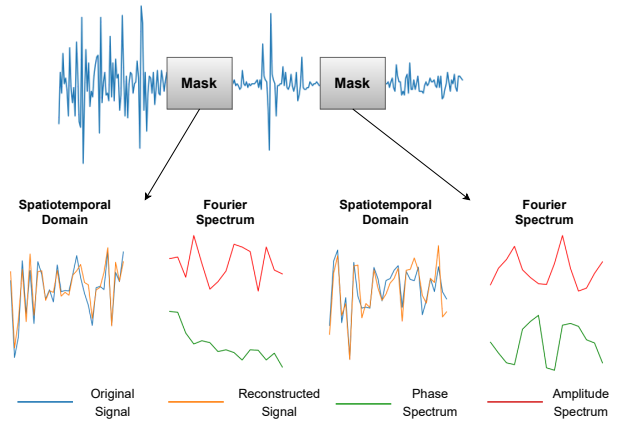


Figure 1: Example of Fourier spectrum prediction on EMG signal. Our model learns to predict the masked signal by predicting the Fourier spectrum of the original signal. For each masked signal segment, we illustrate the original and the predicted signal, as well as the corresponding phase and amplitude of the Fourier spectrum.

rights confirmation email (Conference acronym 'XX). ACM, New York, NY, USA, 10 pages. <https://doi.org/XXXXXXXX.XXXXXXX>

1 INTRODUCTION

Supervised deep learning with million-scale annotated data has witnessed an explosion of success in computer vision (CV) [21, 28] and natural language processing (NLP) [39]. However, such sufficient high-quality annotations are not always available in real-world applications. Learning representations without supervision by leveraging pre-text tasks has become increasingly popular.

In CV, early self-supervised learning approaches [16, 47] aim to capture invariant features through predicting transformations applied to the same image. However, these methods rely on vision ad-hoc heuristics, which are not applicable onto other modalities. More recently, self-supervised contrastive learning approaches witnessed significant progress, even outperforming supervised methods on several downstream tasks. Despite different mechanisms of contrasting, contrastive-based methods learn generic representation by minimizing the distance between two augmented views of the same image in the embedded space. On the other hand, the

underlying idea of self-supervised pre-training for NLP is to first randomly mask out a proportion of tokens within the text and then recover the masked tokens. Autoregressive language modeling as in GPT [38] and masked autoencoding as in BERT [12] enabled state-of-the-art performance in multiple language understanding tasks such as sentiment classification [46], natural language inference [41] and entity recognition [11].

However, unlike CV and NLP, self-supervised pre-training for neurophysiological signals is far from established. Neurophysiological signals are an essential type of data that is ubiquitous in a wide variety of applications, including neurodegenerative disease diagnosis [43, 44], rehabilitation [34], and brain machine interfaces (BCIs). Different from human languages and natural images, neurophysiological signals are far more informatively sparse in the spatiotemporal domain. Thus, learning generic representations for neurophysiological signals via self-supervised training remains challenging. Recently, inspired by the success of contrastive learning, some researchers [15, 45] proposed contrastive based pre-training methods on neurophysiological signals such as electroencephalogram (EEG). The success of contrastive learning relies on two essential assumptions: (i) *augmented views of the same data sample should be semantically consistent in the latent representation space*; (ii) *strong augmentations are required to learn useful representation*. However, these two assumptions are poorly satisfied when the underlying modality changes from images to neurophysiological signals. Among all vision augmentation techniques such as color jittering, *RandomResizedCrop* (RRC) and random grayscale conversion, RRC plays the essential role [42]. RRC first randomly crops a patch at a random location from the image and then resizes the patch to the original image size. No similar cropping and resizing-based augmentation exists for neurophysiological signals. The most commonly adopted augmentation technique for neurophysiological signals is bandpass filtering, where a particular band of frequencies is removed from the original signal. Unfortunately, the filtered signal is not guaranteed to be semantically consistent with the original signal as a useful frequency band might be filtered out. Other augmentations, such as adding random noise and channel flipping, are weak augmentations so as to bring limited improvements in terms of the learned representation. Moreover, augmentations for neurophysiological signals require deliberate hyper-parameter tuning due to the variation of different neurophysiological signals. As reported in [15, 45], the hyper-parameters of augmentations vary from dataset to dataset and from task to task.

To remedy the inadequacy of self-supervised pre-training on neurophysiological signals, we propose *neuro2vec* for self-supervised neurophysiology representation learning. Motivated and inspired by the success of BERT, our approach applies the denoising auto-encoding idea to pre-training of neurophysiology data. In particular, our approach predicts the missing information from either the spatiotemporal domain or the Fourier domain given a masked neurophysiological time sequence. By imputation from frequency and phase, the pre-trained model yields a better understanding of the underlying neurophysiology activities. For instance, the frequency of the EEG signal is a strong indicator of brain activity, while the phase of the EMG signal reflects muscle fiber recruitment patterns. An illustration of the proposed self-supervised neurophysiological pre-training is given in Figure 1. Our approach is intuitively

and practically straightforward. Compared to contrastive-based methods that strongly rely on carefully designed and tuned data augmentations, *neuro2vec* works reasonably well without any augmentations. In this way, we also avoid any potential corrupting of the original data induced by improper augmentations. In terms of network architecture, *neuro2vec* requires no siamese structure as adopted by most contrastive-based methodologies [6, 8, 18].

In summary, our contributions are summarized as follows:

- We propose a transformer-based denoising auto-encoding pre-training method for self-supervised neurophysiological representation learning.
- We investigate missing information imputation in both spatiotemporal and Fourier domain. We show that by asking to predict the frequency and phase component of the signal, the pre-trained model better captures the underlying neurophysiological activities.
- Comprehensive experiments on both EEG and EMG benchmarks show that our proposed pre-training method achieves state-of-the-art performances.

2 RELATED WORK

2.1 Contrastive Learning

Contrastive learning methods learn instance-level discriminative representations by extracting invariant features over distorted views of the same data point. MoCo [20] adopted a large memory bank to introduce enough informative negative samples, while SimCLR [8] adopted a larger batch size to replace the memory bank mechanism. BYOL [18] and its variants [9, 10] further eliminates the requirement of negative samples, using various techniques to avoid representation collapse. Motivated by the success of contrastive learning in CV, some research endeavors are made to adopt contrastive learning onto time series [15, 45]. TS-TCC [15] proposed to contrast time series from both temporal and contextual domains using different augmentation techniques on different views of the signal. In particular, they randomly add noise and re-scale one view of the signal while segmenting, rearranging, and re-scaling the other view as data augmentation. Due to the high variability of neurophysiological signals, applying contrastive learning directly to neurophysiological representation learning inevitably introduces additional hyper-parameters making the augmentation-related parameter tuning a troublesome task. The natural clustering property induced by pulling near similar representations and pushing away dissimilar samples makes the learned representations linearly separable. Linear probing [8] is therefore commonly adopted to evaluate performances of contrastive-based methods. However, it misses the opportunity of learning strong but non-linear features, which limits the power of deep learning. Thus, in this work, we aim to maximize the performance of the model on downstream tasks with an end-to-end fine-tuning protocol [3, 9, 19].

2.2 Autoregressive Modeling

The pioneering work of applying the notion of autoregressive modeling to learn representations is the classic autoencoding [24]. Autoencoders first map the input data to a latent space and then reconstruct the input from the representation in the latent space.

Denosing autoencoders [40] are a family of autoencoders that reconstruct the uncorrupted input signal with a corrupted version of the signal as input. Generalizing the denosing autoregressive modeling, masked predictions attracted the attention of both the NLP and vision community. BERT [12] performs masked language modeling where the task is to predict the randomly masked input tokens. Representations learned by BERT as pre-training generalize well to a variety of downstream tasks. For CV, inpainting tasks [35] to predict large missing regions using convolutional networks is proposed to learn representation. iGPT [7] predicts succeeding pixels given a sequence of pixels as input. MAE [19] and BEiT [3] mask out random patches of the input image and reconstruct the missing patches with a Vision Transformer (ViT). Only visible patches are fed to the encoder in MAE, while both visible and masked patches are fed in BEiT. The most appealing property of autoregressive modeling, compared to contrastive-based methods, is its simplicity and minimal reliance on dataset-specific augmentation engineering.

3 METHOD

Our framework performs masked prediction tasks which inpaint masked neurophysiological content up to some details. In this section, we first discuss the architecture used in our neuro2vec in Section 3.1 and investigate different prediction tasks in both spatiotemporal and Fourier domains in Section 3.3.

3.1 Architecture

Similar to vision, until recently, convolution-based architectures [15, 29, 30] are dominant in the existing domain of neurophysiological applications. Deliberately-designed network structures and data flows are proposed to handle modality-specific tasks. In addition, the spatiotemporal inductive bias imposed by the convolution operation makes CNN-based architectures incapable of directly embracing the techniques used in masked autoencoding such as token masking [12] and positional embedding [39]. To address this issue, we utilize a transformer-based architecture to come up with a unified end-to-end framework that takes raw neurophysiological signals as input.

Our architecture follows the standard transformer architecture with slight modifications. Instead of directly linearly projecting the input data to the model dimension, we use non-overlapping 1-D convolution to encode the input signal into a sequence of segments following the work of Vision Transformers (ViT) [13]. Formally, let $X \in \mathbb{R}^{N \times C}$ be a neurophysiological signal of length N with C channels, a non-overlapping 1-D convolution with kernel size k is applied on X to produce a vector map $v \in \mathbb{R}^{\frac{N}{k} \times d}$. d is the projection dimension. The resulting vector map v could then be viewed as sequence of $\frac{N}{k}$ d -dimensional patches. The convolution operation is followed by a GELU non-linearity [23]. Since the transformer is a feed-forward architecture that does not capture the input temporal order information, we add a learnable positional embedding to each patch embedding. The resulting sequence is then fed into the transformer encoder. The encoder in our framework is used to generate neurophysiological representations. A decoder is only used to perform the denosing reconstruction task during the pre-training phase. Therefore, the decoder architecture can be of arbitrary form independent of the encoder architecture, which is default to a linear

layer. A general illustration of our framework is shown in Fig. 2. We detail the structure in Section 4.

3.2 Masking

Given the sequence of non-overlapping patches v of a neurophysiological signal embedded by the 1-D convolution, we randomly mask a subset of the patches with a masking ratio r following a uniform distribution. During the denosing task pre-training, the masked patches are initialized with a learnable parameter and then input to the transformer encoder.

3.3 Prediction Targets

We consider to denoise the masked input neurophysiological signal from both the spatiotemporal and the Fourier domain:

Spatiotemporal Domain. The no-sweat approach would be to directly reconstruct the amplitude of the masked neurophysiological signal in the spatiotemporal domain following the standard practice of [3, 19]. We first standardize the input neurophysiological signal by subtracting the mean and dividing the standard deviation. Then a mean square error between the decoder's predicted amplitude and the ground truth is adopted as the loss function during training. Human language is a set of extremely semantically rich and information-dense signals. When a model is trained to predict missing words per sentence, this process promotes sophisticated language comprehension both grammatically and semantically. Based on the Markov property of NLP, early methods adopt simple N-gram [5] modeling and work well. Similarly, by using visual information about visible structures, humans are also capable of inpainting the masked regions of an image up to a certain level of detail. On the contrary, due to the apparent stochasticity, nonstationarity, and nonlinearity nature of neurophysiological signals [33], it is deemed difficult to directly inpaint the masked signal in the spatiotemporal domain. To address this issue, we next explore the denosing task in the Fourier domain.

Fourier Domain. Given a discrete neurophysiological signal $X^c = [x_1, x_2, \dots, x_n]$ of channel c , the discrete Fourier transform (DFT) is defined by:

$$X_m = \sum_{n=1}^{n=N} x_n * e^{-\frac{2\pi j}{N} mn}, \quad (1)$$

where $m \in [1, N]$. We further expend Equation (1) into real and imaginary part using the Euler's formula:

$$X_m = \sum_{n=1}^{n=N} x_n * \underbrace{\cos\left(\frac{2\pi}{N} mn\right)}_{real} - j * \underbrace{\sin\left(\frac{2\pi}{N} mn\right)}_{imaginary}, \quad (2)$$

where j is the imaginary unit satisfying $j^2 = -1$. Specifically, X_m represents the spectrum of the sequence x_n at the frequency $\omega_m = 2\pi m/N$. We can then calculate the magnitude $\|X_m\|^2$ and phase θ_m :

$$\|X_m\|^2 = \frac{1}{N} \sqrt{\text{Re}(X_m)^2 + \text{Im}(X_m)^2} \quad (3)$$

$$\theta_m = \text{atan2}(\text{Re}(X_m)^2, \text{Im}(X_m)^2),$$

where $\text{atan2}(\cdot, \cdot)$ is the two-argument arctangent function, Re and Im indicate real and imaginary parts respectively. Next, we elaborate

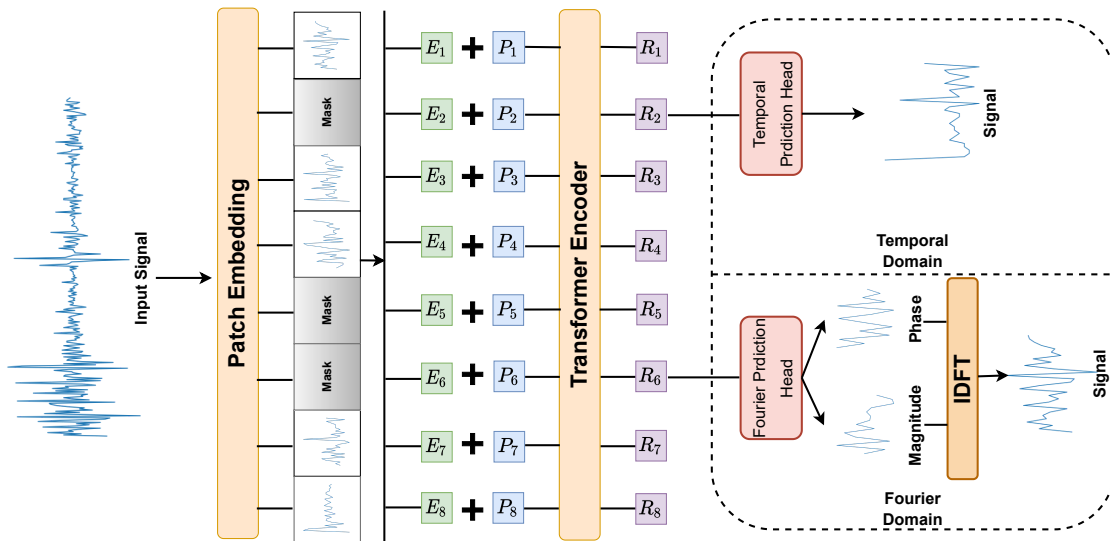


Figure 2: The proposed learning framework for neurophysiological representation learning. The input neurophysiological signal is split into a sequence of patches without overlapping and then projected to a sequence of patch embeddings E with the 1-D convolutional embedding layer. Each patch embedding is added with a learnable positional embedding P and then input to the transformer encoder. The output of the transformer R is used as the neurophysiological patch representation. During self-supervised pre-training, we randomly mask a portion of patches and ask the model to either reconstruct the neurophysiological from the spatiotemporal domain or the Fourier domain. During the pre-training task, the model implicitly learns a useful representation of frequency and phase in the spatiotemporal domain or explicitly via predicting the Fourier spectrum. For downstream tasks, we adopt representation of the classification token and use a linear layer to perform tasks of either classification or regression.

on how magnitude and phase help learn better neurophysiological representations, in particular, electroencephalogram (EEG) and electromyography (EMG). Electrodes pick up the sum of charges from synchronized synaptic activity forming the EEG signal. The surface EEG signal demonstrates oscillations of varying frequencies. Several of these oscillations have characteristic frequencies and correspond to different states of brain activity [25]. EEG signal usually falls into the low frequency range ($<100\text{Hz}$), which are further divided into bandwidths known as delta, theta, alpha, and beta [27]. The alpha band ranging from 8-13 Hz is highly associated with brain maturity and inhibition control which emerges with the closing of the eyes and with relaxation. In a downstream task of sleep stage detection [1], an EEG signal with high alpha band power is an indicator of deep sleep. During active movements, beta band ranging from 13-30 Hz power is generally attenuated, as it is closely linked to motor behavior. **Modeling frequency distribution for representation learning is intrinsically modeling the underlying brain activities.** The human motor behaviors such as walking and talking are accomplished by the muscle contractions. The central and peripheral nervous systems control muscles by varying the activity of the motor units that comprise the muscle. A motor unit, often termed a muscle unit, is composed of a motor neuron and the muscle fibers whose axon innervates. An incoming spike trains of synaptic input travels to a motor neuron and innervates corresponding muscle fibers. Arrival of an action potential from the motor neuron at the neuromuscular junction evokes a large release

Algorithm 1 Pseudocode of Fourier Domain Denoising.

```
# x: masked patch sequence, B x N x C
# X: the discrete Fourier transform of B x (N/2+1) x C
# model : the transformer model
X = rfft2(x, dim=1)
magnitude, phase = model(x)
X_tilde = magnitude * torch.exp(1j * phase)
denoised_x = irfft2(X_tilde, dim=1)
```

rfft/irfft: 1D FFT/IFFT for real signal

of the neurotransmitter, which depolarizes the muscle fiber membrane and generates a muscle unit action potential (MUAP) [22]. Electrodes then pick up the superimposed MUAPs to form the EMG signal. The motor units could be viewed as filters which are often categorized by their amplitude and phase response. Amplitude response can be expressed as a function of frequency, i.e., output amplitude to input. Also, the phase response refers to the phase of the output relative to the input. While the muscle is contracted, it moves longitudinally and transversely based on the fiber direction. The bio-impedance of the motor unit as a filter thus varies, leading to a varying amplitude and phase response. **In other words, by predicting amplitude and phase, the model captures the muscle contraction pattern as representation learning.**

With these bio-inspired motivations in mind, we discuss different strategies for denoising targets in the Fourier domain as follows. The simplest strategy is to directly ask the model to predict the frequency and phase of the masked signal segments. During the

Table 1: Description of used datasets in our experiments.

Datasets	SleepEDF [36]	Epilepsy [2]	Ninapro [37]	
Downstream Task	Classification	Classification	Classification	Regression
Train samples	25612	9200	118403	118403
Test samples	8910	2300	39468	39468
Class number	5	2	18	-
Sequence length	3000	178	50	50
Channel number	1	1	16	16
ConvNet	K=25	K=4	K=8	
Transformer	P=30	P=4	P=4	
Random Scaling	$\sigma = 1.5$	$\sigma = 0.001$	$\sigma = 1.8$	
Random Jittering	M=12	M=5	M=2	
Random Permutation	$\sigma = 2$	$\sigma = 0.001$	$\sigma = 2$	

pre-training, our loss then minimizes the mean square error loss between the predicted and original amplitude and phase of the signal. Also, it should be emphasized that DFT is a one-to-one transformation. With the DFT X_m , the inverse DFT (IDFT) could be used to retrieve the original signal x_n :

$$x_n = \sum_{m=1}^{m=N} X_m * e^{-\frac{2\pi j}{N} mn}. \quad (4)$$

With IDFT, the model is first pre-trained to predict the missing amplitude and phase of the signal, and IDFT is applied to transform the predicted amplitude and phase back into the spatiotemporal domain. Our loss then minimizes the mean square error loss between the inversely transformed signal and the original signal. We provide a pseudo code in Pytorch style in Algorithm 1.

It is worth noting that for real neurophysiological signal input x_n , its DFT is conjugate symmetric, which implies that the half of the DFT contains the complete information about the frequency and phase characteristics of x_n . This reduces the prediction target size by half compared to directly predicting missing information from the spatiotemporal domain. Finally, DFT computation is cheap and introduces negligible overhead by the use of fast Fourier transform (FFT) algorithms which take advantage of the symmetry and periodicity properties of Fourier transform.

4 EXPERIMENTS

This section demonstrates the effectiveness of our proposed pre-training approach; we evaluate our method for EMG and EEG-related applications. In particular, we consider downstream tasks of epileptic seizure detection and sleep stage detection for EEG signals. For EMG signal, we consider the downstream task of hand gesture recognition and finger joint angle regression.

4.1 Datasets

Epileptic Seizure Detection: An epileptic seizure is a period of symptoms resulting from abnormally excessive or synchronized neuronal activity in the brain, which can be detected using EEG signals. The Epileptic Seizure Recognition Dataset [2] contains EEG recordings from 500 subjects consisting of healthy subjects and subjects suffering from epilepsy. For Each subject, 23.6 seconds of brain activity EEG is recorded, then segmented into one-second chunks with annotated labels. The original dataset provides five categories of annotations: EEG recorded with eyes open, EEG recorded with eyes closed, EEG recorded from healthy brain regions, EEG recorded

Table 2: Detailed architecture specifications for ConvNet and Transformer backbones utilized in this work.

	ConvNet	Transformer
Stem	K×1, 32, stride 4	P×1, 128, stride P
Block 1	$\begin{bmatrix} 7\times 1, 64 \\ \text{MaxPool, stride 2} \end{bmatrix} \times 1$	$\begin{bmatrix} \text{MSA, 128, rel. pos.} \\ 1\times 1, 512 \\ 1\times 1, 128 \end{bmatrix} \times 1$
Block 2	$\begin{bmatrix} 7\times 1, 128 \\ \text{MaxPool, stride 2} \end{bmatrix} \times 1$	$\begin{bmatrix} \text{MSA, 128} \\ 1\times 1, 512 \\ 1\times 1, 128 \end{bmatrix} \times 1$
Block 3	$\begin{bmatrix} 7\times 1, 256 \\ \text{MaxPool, stride 2} \end{bmatrix} \times 1$	$\begin{bmatrix} \text{MSA, 128} \\ 1\times 1, 512 \\ 1\times 1, 128 \end{bmatrix} \times 1$
Block 4	$[7\times 1, 512] \times 1$	$\begin{bmatrix} \text{MSA, 128} \\ 1\times 1, 512 \\ 1\times 1, 128 \end{bmatrix} \times 1$
# params.	1.22×10^6 (K=4)	0.798×10^6 (P=4)

from tumor brain regions, and EEG recorded during seizure onset. We follow most works where the previous four categories are merged and classified against the last category of seizure onset.

Sleep Stage Recognition: Human sleep can be divided into the following five stages: Wake (W), Non-rapid eye movement (N1, N2, N3), and Rapid Eye Movement (REM). The Sleep-EDF Dataset [36] contains EEG recordings from Caucasian males and females (21–35 years old) without any medication. The EEG signal is required at a sampling rate of 100 HZ. Following previous studies [14, 15], we utilize the Fpz-Cz channel in this study. The EEG recordings are segmented into 10-second windows.

Hand Gesture Recognition: Humans perform finger and wrist movements by contracting muscles of the forearm. The Ninapro DB5 Dataset [37] contains EMG signals collected from 10 intact subjects using 16 active single-differential wireless electrodes. Each subject wears two armbands closed to the elbow during data acquisition. DB5 contains three exercises for each subject: (1) Basic finger movements, (2) Isometric and isotonic hand movements, as well as basic wrist movements, and (3) Grasping and functional movements. During each exercise, the subjects are required to repeat each movement six times with rest in between to avoid muscle fatigue. In our experiment, we randomly pick five repetitions as the training set and the remaining one as the testing set. We choose exercise (2), which contains 17 different gestures within this work. The EMG recordings are segmented using a sliding window method with window size 50 and stride five.

Finger Joint Angle Regression: For the task of finger joint angle regression, we also use the Ninapro DB5 Dataset [37]. Besides categorical labels of all three exercises in DB5, each subject is asked to wear a data glove to collect finger joint kinematic information during EMG acquisition. There are, in total, 22 sensors placed on the glove. Since the abduction and adduction movement of the fingers is associated with muscle located in the palm, we remove these sensors from this study and only choose sensors that reflect the finger joint angle during the extension and flexion movement of the fingers. In particular, we pick the sensors placed at The distal

Table 3: Comparison with previous self-supervised methods on SleepEDF and Epilepsy datasets. Acc (%), mAP (%), and macro F1 (%) for linear and fine-tuning evaluations are reported.

Methods	Pre-training	Backbone	SleepEDF				Epilepsy			
			kNN (Acc)↑	SVM (mAP)↑	FT (Acc)↑	FT (F1)↑	kNN (Acc)↑	SVM (mAP)↑	FT (Acc)↑	FT (F1)↑
Rand. init.	Random	ConvNet	65.82±4.96	69.15±4.14	83.34±0.42	76.71±0.65	90.13±3.56	97.52±4.35	97.46±0.26	95.61±0.42
AttnSleep [14]	Supervised	ConvNet	-	-	84.23±0.56	77.84±0.74	-	-	97.35±0.31	94.54±0.57
SimCLR [8]	Contrastive	ConvNet	72.47±0.84	75.47±0.68	83.60±0.79	76.96±0.89	95.28±0.56	96.09±0.64	97.52±0.41	95.98±0.76
BYOL [18]	Contrastive	ConvNet	71.65±0.73	75.26±0.81	83.29±0.76	76.68±0.94	94.54±0.48	96.64±0.52	97.94±0.64	96.70±0.87
SwAV [6]	Contrastive	ConvNet	76.19±1.24	76.83±1.56	83.84±1.35	77.18±1.62	95.95±1.23	98.36±1.43	98.60±1.12	97.82±0.53
MoCo.V3 [10]	Contrastive	ConvNet	72.53±0.75	75.51±0.84	83.46±0.68	76.70±0.76	94.33±0.31	95.09±0.34	98.74±0.58	97.98±0.64
TS-TCC [15]	Contrastive	ConvNet	73.87±0.76	76.12±0.98	84.05±0.82	77.04±0.88	96.98±0.35	98.74±0.37	98.75±0.78	97.81±0.72
Rand. init.	Random	Transformer	66.75±4.10	69.50±3.26	84.20±0.41	77.15±0.59	90.23±3.74	96.29±4.03	97.88±0.27	96.54±0.38
MoCo.V3 [10]	Contrastive	Transformer	75.61±0.63	77.84±0.82	85.49±0.72	77.73±0.80	98.17±0.34	98.91±0.42	98.93±0.59	98.60±0.58
MAE [19]	Autoregressive	Transformer	68.43±0.89	70.78±0.94	85.08±0.89	77.40±0.86	90.64±0.49	96.95±0.59	99.15±0.74	98.79±0.64
neuro2vec	Autoregressive	Transformer	69.55±0.82	71.49±0.84	86.53±0.83	78.94±0.87	93.78±0.47	97.06±0.57	99.34±0.66	98.82±0.65

Table 4: Comparison with previous works for classification and regression tasks on Ninapro DB5 dataset. Acc (%), mAP (%), macro F1 (%), MSE (10^{-2}), and MAE (10^{-2}) for linear and fine-tuning evaluations are reported.

Methods	Pre-training	Backbone	Ninapro (Classification)				Ninapro (Regression)	
			kNN (Acc)↑	SVM (mAP)↑	FT (Acc)↑	FT (F1)↑	FT(MSE)↓	FT(MAE)↓
Rand. init.	Random	ConvNet	64.69 ±5.79	10.61 ±3.43	91.21 ±0.52	80.35 ±0.89	5.61 ±0.54	63.38 ±2.57
SimAttn [26]	Supervised	ConvNet	-	-	89.15±0.67	78.96±0.78	5.73±0.66	63.32±2.63
SimCLR [8]	Contrastive	ConvNet	87.14 ±0.82	65.86 ±0.87	91.73 ±0.75	80.86 ±0.67	5.54 ±0.57	63.50 ±1.64
BYOL [18]	Contrastive	ConvNet	85.57 ±0.87	66.02 ±0.96	91.56 ±0.84	80.69 ±0.95	5.72 ±0.45	63.74 ±1.97
SwAV [6]	Contrastive	ConvNet	86.13 ±2.33	64.43 ±2.12	91.84 ±1.76	81.07 ±2.45	5.78 ±0.65	63.32 ±2.20
MoCo.V3 [10]	Contrastive	ConvNet	87.45 ±0.66	66.29 ±0.78	92.14 ±0.66	81.45 ±0.78	5.46 ±0.39	62.83 ±1.92
TS-TCC [15]	Contrastive	ConvNet	86.87 ±0.95	66.10 ±0.93	92.02 ±0.95	80.93 ±1.12	5.14 ±0.40	62.95 ±1.83
Rand. init.	Random	Transformer	65.28 ±4.73	11.07 ±4.51	91.97 ±0.58	81.46 ±0.56	5.28 ±0.48	61.21 ±1.93
MoCo.V3 [10]	Contrastive	Transformer	89.01 ±0.71	69.34 ±0.74	92.15 ±0.71	83.23 ±0.72	5.57 ±0.51	62.38 ±2.04
MAE [19]	Autoregressive	Transformer	77.53 ±0.84	48.67 ±0.82	93.03 ±0.78	84.32 ±0.82	5.03 ±0.45	60.79 ±1.71
neuro2vec	Autoregressive	Transformer	79.38 ±0.82	53.25 ±0.84	94.28±0.72	86.69±0.78	4.72±0.43	60.11±1.46

interphalangeal (DIP) joint and metacarpophalangeal (MCP) for the thumb and sensors placed at DIP, proximal interphalangeal (PIP), and MCP for the remaining four fingers. The joint angle data is normalized for each sensor respectively. We adopt exercise (1) for this task, which contains 12 fine finger gestures. The recordings are segmented the same way we described for the hand gesture recognition task. We calculate and adopt the mean of joint angle for each EMG window as prediction label.

4.2 Experimental Setup

Evaluation Protocols: Each dataset is randomly split into 80% and 20% for training and testing, while we further split 20% of the training data for validation purposes. We perform five trials for each task with five different random seeds and report the mean and standard deviation of all metrics. In specific, we report top-1 accuracy (Acc), mean average precision (mAP), and macro-averaged F1-score (macro F1) for classification tasks. Note that mAP and macro F1 could better evaluate the classification performance given imbalanced datasets. For the regression tasks, we report the mean absolute error (MAE) and mean squared error (MSE). Following linear protocols in contrastive learning [17], we evaluate the discrimination abilities of learned representations by training kNN classifiers ($k = 20$) and linear SVMs [4] (*one-vs-all*) on the frozen features. Following the commonly adopted fine-tuning (FT) protocol [17, 19] for fully-supervised and semi-supervised scenarios,

we fine-tune the full model for 40 epochs on labeled data. Our main focus is to learn representations with better fine-tuning performances, which can make full use of strong non-linear features. Table 1 summarizes statistics and settings of all datasets.

Baseline Methods: We consider two strands of self-supervised methods as baseline methods, namely *contrastive-learning* based methods and *autoregressive* based methods. Without loss of generality, for contrastive-based methods, we choose methods that utilize both positive and negative samples, SimCLR [8], SwAV [6], and MoCo.V3 [10]; we also consider methods that only require positive sample pairs, BYOL [18]. We compare the results of MoCo.V3 using both CNN and transformer architectures since it is compatible with both CNN and transformer architectures. Additionally, we pick TS-TCC [15] which is a contrastive-based method designed for time series pre-training as a competitive baseline. For autoregressive-based method, we choose MAE [19]. Besides the aforementioned methods, we also consider state-of-the-art supervised methods, SimAttn [26] for EMG tasks and AttnSleep [14] for EEG tasks. We provide supervised training results with random weight initialization of CNN and transformer backbones in Table 2 for reference.

Network Architectures: We adopt a simple yet effective plain convolution network architecture (ConvNet) as the backbone for all contrastive-based baseline methods, which is detailed in the left column of Table 2. ConvNet contains a stem layer that contains a

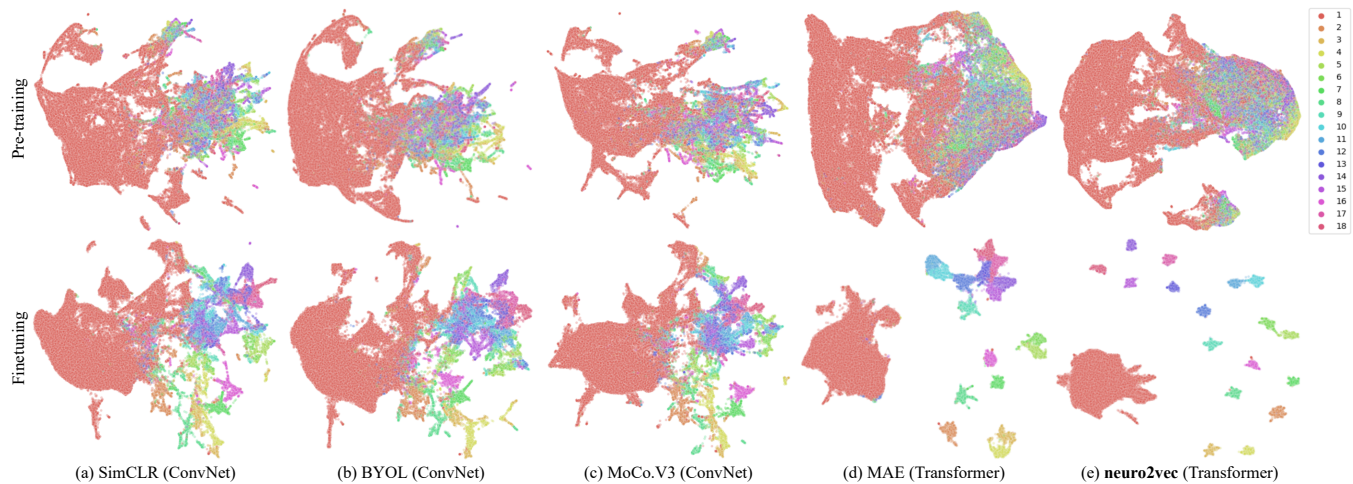


Figure 3: Visualization of pre-trained and fine-tuned embeddings with UMAP of hand gesture classification task on the Ninapro dataset. The first row shows the visualization of embeddings after pre-training, while the second row shows the visualization of embeddings after fine-tuning. Contrastive learning based methods demonstrate better discrimination ability after fine-tuning than MAE and our proposed method. However, fine-tuning contrastive-based methods brings limited improvement while for autoregressive-based methods such as MAE and our proposed methods gain huge improvement from fine-tuning.

1-D convolution layer with the kernel size of $K \times 1$, the stride of 4, and the output channels of 32. The number of input channels C and the kernel size K is adjusted for each dataset, as shown in Table 4.1. Each convolution block consists of a 1-D convolution layer (followed by a batch normalization layer and a ReLU activation) and a max pooling layer. For simplicity, we fix the convolution kernel size in each block and double the number of output channels concerning the previous block. Then we adopt a global average pooling layer and a fully connected layer to map the output of the last block to fit the pre-training or the actual downstream tasks. Notice that all contrastive-based methods adopt an additional 2-layer MLP projector or predictor during pre-training as the original paper with the hidden dimension of 1024. For the transformer backbone, as illustrated in the right column of Table 2, we perform patch embedding by a 1-D convolution layer with the kernel size of $P \times 1$ and the number of output channels of 128, which is adjusted in each dataset as in Table 1. The stride is also set to P to ensure non-overlapping patch embedding [12, 13]. Following the stem layer are four blocks consisting of multi-head self-attention (MSA) with relative positional encoding (rel. pos.). We adopt the regular MSA structure with pre-normalization and residual connection as in ViT [13]. The hidden dimension of the Feed Forward Network (FFN) is set to a fixed value of 512. We adopt the representation learned from the classification token and apply a fully connected layer for the pre-training or the actual downstream tasks in the case of the transformer. For impartial comparison, ConvNet and Transformer used in our experiments have a similar number of parameters in total (as shown in the last line of Table 2) and yield similar performances.

Implementation Details: We adopt AdamW [31] as the optimizer with weight decay of $1e-2$, $\beta_1 = 0.9$, $\beta_2 = 0.999$ and Cosine learning rate scheduler for all experiments. For pre-training, we use a batch size of 256, a basic learning rate of $3e-3$, and a dropout rate of 0.1; for fine-tuning and supervised learning baselines, we apply the

batch size of 128, the learning rate of $3e-4$, and the dropout rate of 0.3 and 0.2 for ConvNet and Transformer, respectively. As for data augmentation strategies for contrastive-based methods, we adopt three types of time-series augmentations as [15], *Random Scaling* by Gaussian noise with σ , *Random Jittering* by Gaussian noise with σ , *Random permutation* of a random number of segments with a maximum of M . Detailed augmentation settings for each dataset are provided in Table 1. Note that pre-training of Transformer and fine-tuning do not require any data augmentation. By default, we adopt the IDFT output of the predicted Fourier spectrum as predicting target and provide ablation studies on other targets in Section 4.4.

4.3 Comparison Results

Fine-tuning and Linear Evaluation Results: We first evaluate the performance of the proposed neuro2vec in comparison to current self-supervised methods. We aim to maximize the performance of the model on downstream tasks with an end-to-end fine-tuning protocol (FT) which is more practical than the linear evaluations (kNN and SVM) in real-world scenarios. As shown in Table 3 and Table 4, neuro2vec significantly outperforms both the supervised and self-supervised pre-training methods for classification tasks on SleepEDF, Epilepsy, and Ninapro datasets. Compared to contrastive-based methods, neuro2vec brings more fine-tuning performance gains over the random initialization than current state-of-the-art contrastive methods: +2.33% Acc and +1.79% macro F1 for neuro2vec v.s. +0.71% Acc and +0.33% macro F1 for TS-TCC on SleepEDF, +2.31% Acc and +5.23% macro F1 for neuro2vec v.s. +0.18% Acc and +1.77% macro F1 for MoCo.V3 on Ninapro. Next, we also investigate linear evaluation, which is commonly adopted for contrastive-based methods. Note that we only report FT results of supervised methods since the whole network is trained with labels where linear protocol is not applicable. We observe that contrastive-based methods outperform autoregressive based methods due to

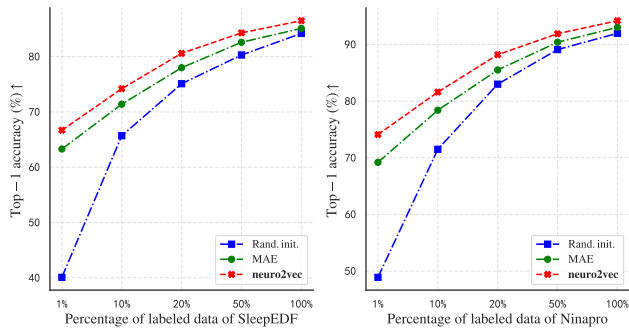


Figure 4: Acc (%) of fine-tuning for semi-supervised scenarios on SleepEDF and Ninapro datasets in comparison of self-supervised pre-training and the random initialization.

their superior discrimination abilities induced by the natural clustering effect. However, contrastive-based methods perform way worse than autoregressive based methods under FT. We argue that the discrimination ability comes with a cost of discarding essential information during pre-training and thus largely limits the performance gain during fine tuning, which is also supported by the visualization results of learned embeddings before the classification head using UMAP [32] in Figure 3. On the contrary, autoregressive methods as our proposed neuro2vec and MAE capture low-level features and thus learn more general representations, which are more generic for various downstream tasks. Compared to the autoregressive method, neuro2vec noticeably outperforms fine-tuning performances of MAE by 0.19~1.45% Acc and 0.03~2.37% macro F1. Meanwhile, neuro2vec also achieves the best performance for the finger joint angle regression task on Ninapro dataset in Table 4. Overall, our proposed neuro2vec achieves state-of-the-art performances for neurophysiological representation learning.

Semi-supervised Learning: We then investigate the effectiveness of our neuro2vec under the semi-supervised settings, by training with 1%, 10%, 20%, 50% of randomly selected labeled samples of the training data. As shown in Figure 4, compared with the random initialization (blue curves) and MAE (green curves), neuro2vec (red curves) steadily outperforms them on both SleepEDF and Ninapro datasets. We observe that the random initialization with randomly initialized parameters yields poor performances with limited labeled data (e.g., 1% and 10%). At the same time, our neuro2vec pre-training significantly improves the fine-tuning results in these cases (e.g., +30.31% over the random initialization and +4.93% over MAE using 1% labeled data on Ninapro).

Transfer Learning: We further investigate the transfer ability of neuro2vec by fine-tuning pre-trained models in between the classification task and the regression task on the Ninapro dataset. As shown in Figure 5, neuro2vec yields better performances and smaller transferring gaps than the random initialization and current self-supervised methods based on transformer.

4.4 Ablation Studies

Ablation studies are performed on the SLEEP-EDF dataset with the same experimental setup as described in Section 4.2. We report 40-epoch fine-tuning accuracy (%) on SLEEP-EDF. We study the

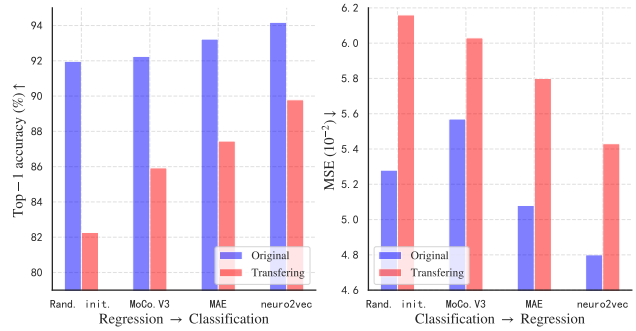


Figure 5: Transfer learning of pre-training on classification and regression subsets of Ninapro datasets in comparison of self-supervised pre-training and the random initialization.

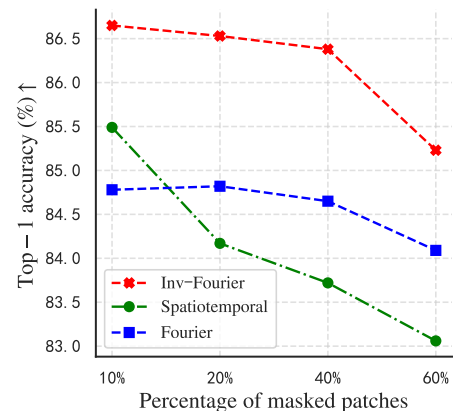


Figure 6: Ablation of masked patches in spatiotemporal and Fourier domains in terms of fine-tuning Acc (%) on SleepEDF.

effects of masking ratio with respect to different prediction targets, namely in spatialtemporal domain and Fourier domain in Figure 6. We consider directly predicting the Fourier spectrum (Fourier) and the transformed spatialtemporal signal of IDFT (Inv-Fourier) using the predicted Fourier spectrum as targets. For Inv-Fourier, we observe that masking ratios of 20% to 40% can produce similar fine-tuning accuracy. For masking ratios of 10% and 60%, these masking ratio leads to degraded performance. For directly predicting Fourier spectrum as target, we observe that the performance is relatively stable under various masking ratios and worse performance than Inv-Fourier. For the spatiotemporal domain, we observe that the best performance is given with a masking ratio of 10%. However, with a masking ratio of 20% and more, we observe a degrading trend in the performance. This indicates that neurophysiological signals are informatively sparse in the spatiotemporal domain, and thus performing autoregressive prediction in the spatiotemporal domain would thus be a very improper and redundant task as modeling the stochasticity and nonstationarity of neurophysiological signals. However, our proposed neuro2vec is simple yet effective through predicting the Fourier spectrum. In conclusion, it is observed that our proposed neuro2vec in Fourier domain outperforms the performance of autoregressive prediction in the spatiotemporal domain.

5 CONCLUSION

In this paper, we present neuro2vec, a self-supervised pre-training approach for neurophysiological signals based on masked Fourier spectrum prediction. We note that neurophysiological signals are of a different nature to images and languages and this difference must be addressed carefully. We analyze in depth that amplitude and phase distribution of Fourier spectrum have strong links to the underlying neural activities. During pre-training, the model first predicts the Fourier spectrum of the masked signal and then reconstructs the original signal in spatiotemporal domain via IDFT. Extensive experiments on EEG and EMG datasets for various downstream applications demonstrate the extraordinary performance of our model compared with various competitive models. Additionally, neuro2vec is efficient and doesn't require carefully designed and tuned data augmentations as contrastive learning methods.

REFERENCES

- [1] Khald Ali I Aboalayon, Miad Faezipour, Wafaa S Almuhammadi, and Saeid Moslehpour. 2016. Sleep stage classification using EEG signal analysis: a comprehensive survey and new investigation. *Entropy* 18, 9 (2016), 272.
- [2] Ralph G Andrzejak, Klaus Lehnertz, Florian Mormann, Christoph Rieke, Peter David, and Christian E Elger. 2001. Indications of nonlinear deterministic and finite-dimensional structures in time series of brain electrical activity: Dependence on recording region and brain state. *Physical Review E* 64, 6 (2001), 061907.
- [3] Hangbo Bao, Li Dong, and Furu Wei. 2021. Beit: Bert pre-training of image transformers. *arXiv preprint arXiv:2106.08254* (2021).
- [4] Bernhard E. Boser, Isabelle Guyon, and Vladimir Naumovich Vapnik. 1992. A training algorithm for optimal margin classifiers. In *COLT '92*.
- [5] Andrei Z Broder, Steven C Glassman, Mark S Manasse, and Geoffrey Zweig. 1997. Syntactic clustering of the web. *Computer networks and ISDN systems* 29, 8-13 (1997), 1157–1166.
- [6] Mathilde Caron, Ishan Misra, Julien Mairal, Priya Goyal, Piotr Bojanowski, and Armand Joulin. 2020. Unsupervised learning of visual features by contrasting cluster assignments. *Advances in Neural Information Processing Systems* 33 (2020), 9912–9924.
- [7] Mark Chen, Alec Radford, Rewon Child, Jeffrey Wu, Heewoo Jun, David Luan, and Ilya Sutskever. 2020. Generative pretraining from pixels. In *International Conference on Machine Learning*. PMLR, 1691–1703.
- [8] Ting Chen, Simon Kornblith, Mohammad Norouzi, and Geoffrey Hinton. 2020. A Simple Framework for Contrastive Learning of Visual Representations. *arXiv preprint arXiv:2002.05709* (2020).
- [9] Xinlei Chen and Kaiming He. 2020. Exploring Simple Siamese Representation Learning. *arXiv preprint arXiv:2011.10566* (2020).
- [10] Xinlei Chen, Saining Xie, and Kaiming He. 2021. An empirical study of training self-supervised vision transformers. In *Proceedings of the IEEE/CVF International Conference on Computer Vision*. 9640–9649.
- [11] Ronan Collobert and Jason Weston. 2008. A Unified Architecture for Natural Language Processing: Deep Neural Networks with Multitask Learning. In *Proceedings of the 25th International Conference on Machine Learning (Helsinki, Finland) (ICML '08)*. Association for Computing Machinery, New York, NY, USA, 160–167.
- [12] Jacob Devlin, Ming-Wei Chang, Kenton Lee, and Kristina Toutanova. 2018. Bert: Pre-training of deep bidirectional transformers for language understanding. *arXiv preprint arXiv:1810.04805* (2018).
- [13] Alexey Dosovitskiy, Lucas Beyer, Alexander Kolesnikov, Dirk Weissenborn, Xiuhua Zhai, Thomas Unterthiner, Mostafa Dehghani, Matthias Minderer, Georg Heigold, Sylvain Gelly, et al. 2020. An image is worth 16x16 words: Transformers for image recognition at scale. *arXiv preprint arXiv:2010.11929* (2020).
- [14] Emadelddeen Eldele, Zhenghua Chen, Chengyu Liu, Min Wu, Chee-Keong Khoo, Xiaoli Li, and Cuntai Guan. 2021. An attention-based deep learning approach for sleep stage classification with single-channel eeg. *IEEE Transactions on Neural Systems and Rehabilitation Engineering* 29 (2021), 809–818.
- [15] Emadelddeen Eldele, Mohamed Ragab, Zhenghua Chen, Min Wu, Chee Keong Khoo, Xiaoli Li, and Cuntai Guan. 2021. Time-Series Representation Learning via Temporal and Contextual Contrasting. In *Proceedings of the Thirtieth International Joint Conference on Artificial Intelligence, IJCAI-21*. 2352–2359.
- [16] Spyros Gidaris, Praveer Singh, and Nikos Komodakis. 2018. Unsupervised representation learning by predicting image rotations. In *International Conference on Learning Representations (ICLR)*.
- [17] Priya Goyal, Dhruv Mahajan, Abhinav Gupta, and Ishan Misra. 2019. Scaling and Benchmarking Self-Supervised Visual Representation Learning. In *Proceedings of the IEEE/CVF International Conference on Computer Vision (ICCV)*.
- [18] Jean-Bastien Grill, Florian Strub, Florent Altché, Corentin Tallec, Pierre H Richemond, Elena Buchatskaya, Carl Doersch, Bernardo Avila Pires, Zhaohan Daniel Guo, Mohammad Gheshlaghi Azar, et al. 2020. Bootstrapping your own latent: A new approach to self-supervised learning. In *NeurIPS*.
- [19] Kaiming He, Xinlei Chen, Saining Xie, Yanghao Li, Piotr Dollár, and Ross Girshick. 2021. Masked autoencoders are scalable vision learners. *arXiv preprint arXiv:2111.06377* (2021).
- [20] Kaiming He, Haoqi Fan, Yuxin Wu, Saining Xie, and Ross Girshick. 2020. Momentum contrast for unsupervised visual representation learning. In *Proceedings of the IEEE/CVF Conference on Computer Vision and Pattern Recognition*. 9729–9738.
- [21] Kaiming He, Xiangyu Zhang, Shaoqing Ren, and Jian Sun. 2016. Deep residual learning for image recognition. In *Proceedings of the IEEE conference on computer vision and pattern recognition*. 770–778.
- [22] CJ Heckman and Roger M Enoka. 2004. Physiology of the motor neuron and the motor unit. In *Handbook of Clinical Neurophysiology*. Vol. 4. Elsevier, 119–147.
- [23] Dan Hendrycks and Kevin Gimpel. 2016. Bridging nonlinearities and stochastic regularizers with gaussian error linear units. (2016).
- [24] Geoffrey E Hinton and Richard Zemel. 1993. Autoencoders, minimum description length and Helmholtz free energy. *Advances in neural information processing systems* 6 (1993).
- [25] Alice F Jackson and Donald J Bolger. 2014. The neurophysiological bases of EEG and EEG measurement: A review for the rest of us. *Psychophysiology* 51, 11 (2014), 1061–1071.
- [26] David Josephs, Carson Drake, Andy Heroy, and John Santerre. 2020. sEMG gesture recognition with a simple model of attention. In *Machine Learning for Health*. PMLR, 126–138.
- [27] Elif Kirmizi-Alsan, Zubeyir Bayraktaroglu, Hakan Gurvit, Yasemin H Keskin, Murat Emre, and Tamer Demiralp. 2006. Comparative analysis of event-related potentials during Go/NoGo and CPT: decomposition of electrophysiological markers of response inhibition and sustained attention. *Brain research* 1104, 1 (2006), 114–128.
- [28] Alex Krizhevsky, Ilya Sutskever, and Geoffrey E Hinton. 2012. ImageNet Classification with Deep Convolutional Neural Networks. In *Advances in Neural Information Processing Systems*, F. Pereira, C. J. C. Burges, L. Bottou, and K. Q. Weinberger (Eds.), Vol. 25. Curran Associates, Inc. <https://proceedings.neurips.cc/paper/2012/file/c399862d3b9d6b76c8436e924a68c45b-Paper.pdf>
- [29] Vernon J Lawhern, Amelia J Solon, Nicholas R Waytowich, Stephen M Gordon, Chou P Hung, and Brent J Lance. 2018. EEGNet: a compact convolutional neural network for EEG-based brain-computer interfaces. *Journal of neural engineering* 15, 5 (2018), 056013.
- [30] Rui Li, Yiting Wang, and Bao-Liang Lu. 2021. *A Multi-Domain Adaptive Graph Convolutional Network for EEG-Based Emotion Recognition*. Association for Computing Machinery, New York, NY, USA, 5565–5573.
- [31] Ilya Loshchilov and Frank Hutter. 2019. Decoupled Weight Decay Regularization. In *International Conference on Learning Representations (ICLR)*.
- [32] Leland McInnes, John Healy, and James Melville. 2018. Umap: Uniform manifold approximation and projection for dimension reduction. *arXiv preprint arXiv:1802.03426* (2018).
- [33] Frank Moss, Lawrence M Ward, and Walter G Sannita. 2004. Stochastic resonance and sensory information processing: a tutorial and review of application. *Clinical neurophysiology* 115, 2 (2004), 267–281.
- [34] Marcello Mulas, Michele Folgheraiter, and Giuseppina Gini. 2005. An EMG-controlled exoskeleton for hand rehabilitation. In *9th International Conference on Rehabilitation Robotics, 2005. ICORR 2005*. IEEE, 371–374.
- [35] Deepak Pathak, Philipp Krahenbuhl, Jeff Donahue, Trevor Darrell, and Alexei A Efros. 2016. Context encoders: Feature learning by inpainting. In *Proceedings of the IEEE conference on computer vision and pattern recognition*. 2536–2544.
- [36] PhysioToolkit PhysioBank. 2000. PhysioNet: components of a new research resource for complex physiologic signals. *Circulation* 101, 23 (2000), e215–e220.
- [37] Stefano Pizzolato, Luca Tagliapietra, Matteo Cognolato, Monica Reggiani, Henning Müller, and Manfredo Atzori. 2017. Comparison of six electromyography acquisition setups on hand movement classification tasks. *PLoS one* 12, 10 (2017), e0186132.
- [38] Alec Radford, Karthik Narasimhan, Tim Salimans, and Ilya Sutskever. 2018. Improving language understanding by generative pre-training (2018).
- [39] Ashish Vaswani, Noam Shazeer, Niki Parmar, Jakob Uszkoreit, Llion Jones, Aidan N Gomez, Łukasz Kaiser, and Illia Polosukhin. 2017. Attention is all you need. *Advances in neural information processing systems* 30 (2017).
- [40] Pascal Vincent, Hugo Larochelle, Isabelle Lajoie, Yoshua Bengio, Pierre-Antoine Manzagol, and Léon Bottou. 2010. Stacked denoising autoencoders: Learning useful representations in a deep network with a local denoising criterion. *Journal of machine learning research* 11, 12 (2010).
- [41] Alex Wang, Amanpreet Singh, Julian Michael, Felix Hill, Omer Levy, and Samuel Bowman. 2018. GLUE: A Multi-Task Benchmark and Analysis Platform for Natural Language Understanding. In *Proceedings of the 2018 EMNLP Workshop BlackboxNLP: Analyzing and Interpreting Neural Networks for NLP*. Association for Computational Linguistics, Brussels, Belgium, 353–355.
- [42] Di Wu, Siyuan Li, Zelin Zang, Kai Wang, Lei Shang, Baigui Sun, Hao Li, and Stan Z Li. 2021. Align Yourself: Self-supervised Pre-training for Fine-grained Recognition via Saliency Alignment. *arXiv preprint arXiv:2106.15788* (2021).
- [43] Di Wu, Yi Shi, Ziyu Wang, Jie Yang, and Mohamad Sawan. 2021. C² SP-Net: Joint Compression and Classification Network for Epilepsy Seizure Prediction. *arXiv preprint arXiv:2110.13674* (2021).
- [44] Di Wu, Jie Yang, and Mohamad Sawan. 2022. Bridging the Gap Between Patient-specific and Patient-independent Seizure Prediction via Knowledge Distillation. *arXiv preprint arXiv:2202.12598* (2022).
- [45] Qinfeng Xiao, Jing Wang, Jianan Ye, Hongjun Zhang, Yuyan Bu, Yiqiong Zhang, and Hao Wu. 2021. Self-Supervised Learning for Sleep Stage Classification with Predictive and Discriminative Contrastive Coding. In *ICASSP 2021 - 2021 IEEE International Conference on Acoustics, Speech and Signal Processing (ICASSP)*. 1290–1294.
- [46] Heng Yang, Biqing Zeng, JianHao Yang, Youwei Song, and Ruyang Xu. 2021. A multi-task learning model for chinese-oriented aspect polarity classification and aspect term extraction. *Neurocomputing* 419 (2021), 344–356.
- [47] Richard Zhang, Phillip Isola, and Alexei A Efros. 2016. Colorful image colorization. In *Proceedings of the European Conference on Computer Vision (ECCV)*.